

# MODELLING OF SPACE CHARGE AND CSR EFFECTS IN BUNCH COMPRESSION SYSTEMS

M. Dohlus, DESY, Hamburg, Germany

## Abstract

Bunches with high peak currents of the order of kilo-Amperes are required in linac based X-ray free electron lasers. These bunches cannot be produced directly in guns because space charge forces would destroy the brilliance within a short distance. Therefore bunches with a peak current of a few tens of Amperes are created in laser-driven radio-frequency sources and are compressed in length by two orders of magnitude. In most designs, the compression is achieved in magnet chicanes, where particles with different energies have different path lengths, so that a bunch with an energy distribution correlated with longitudinal particle position can shrink in length. The principle problem is that short bunches on curved trajectories will emit coherent synchrotron radiation (CSR). CSR effects and space charge fields play an important role in the particle dynamic and the design of a bunch compression system. The presentation will provide an overview of computational methods and simulation tools for coherent synchrotron radiation and space charge effects in magnetic bunch compression systems.

## INTRODUCTION

The essential differences between magnetic bunch compression systems and conventional linear accelerating sections are the presence of dispersive sections and a strong correlation between energy and longitudinal position in a bunch. This leads to the desired bunch compression. During the compression process not only the longitudinal shape but also the transverse dimensions are dramatically changed. This is shown in Fig. 1 with the comparison of a calculation with and without self-interaction. The color of the particles stands for their energy and is changed due to the radiation of coherent synchrotron light in the lower sequence of plots. The transverse widening and shrinking during the compression can be much stronger than in that example; the growth of transverse emittance for a well designed system is less severe. Space charge effects per length scale with  $I/\gamma^2$  but the integrated effects in an accelerator from  $\gamma_1$  to  $\gamma_2 \gg \gamma_1$  are proportional to  $I/\gamma_1 \cdot \ln(\gamma_2/\gamma_1)$ . The ratio  $I/\gamma_1$  after compression is increased to values typically for injection systems where space charge effects are important.

Two operational modes ('rollover compression' and 'controlled compression' with higher harmonic rf) are presently used [1] or proposed [2]. Part II of this paper gives examples for both modes and demonstrates that in any case effects due to space charge and coherent synchrotron radiation contribute significantly to the particle dynamics. Therefore this second part is devoted to problems of realistic simulations of bunch compression systems. As a variety of effects (SC, CSR, wakes, rf and

non-linearities) have to be considered and usually more than one tracking code is needed. We distinguish two type of tracking problems. For the first, the trajectory is approximately linear and the length scale of shape variations (e.g. due to betatron motion) is large compared to the build up time of electromagnetic fields. Codes for that type of problems are well developed and are not discussed here.

A new class of beam dynamics codes is required for non-linear trajectories and shape variant distributions where coherent radiation effects are not negligible and the length scale of transients is of the same order as the length scale on which shape variations take place. These codes are usually called CSR codes although the name stands only for one of several physical mechanisms that have to be considered. Part I of this report gives an overview of approaches for that purpose.

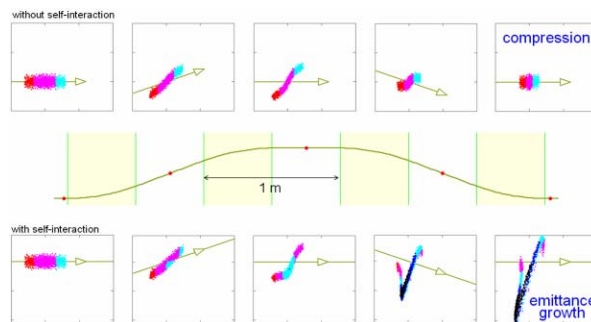


Fig. 1: Shape variation during compression.

## PART I: CSR CODES

A basic classification of methods for the numerical calculation of electromagnetic fields distinguishes whether the field-filled-volume is discretized or not. Methods with volume discretization are usually based on solving partial differential equations (PDE) and the grid resolution has to be sufficient to avoid dispersion errors of numerical wave propagation. The discretized volume is limited in space and therefore bounded, e.g., by a perfect electric conducting (PEC) surface. The other type solves the field by integration of all retarded sources. The natural boundary condition is free space (or 'open'). Lorentz forces and electromagnetic fields are calculated directly at the locations where they are needed by integration of a comparatively small volume of retarded sources. But this integration has to be repeated for each new observer point and there is no advantage from the knowledge of field values in the past. Therefore the effort for a completely new field calculation in a small volume of interest has to be compared with the efficiency of time stepping algorithms that treat an extremely large volume (with respect to the bunch dimensions).

### Vlasov-Maxwell-Approach

Bassi et al. [3,4] study CSR for arbitrary planar orbits based on a fully self-consistent Vlasov-Maxwell treatment. The main motivation is that the Vlasov approach will be less sensitive to spatial noise than the standard particle approaches.

The phase space distribution is represented by a 4d density  $f(z, p_z, x, p_x, s)$  in the beam frame with the horizontal coordinates  $z, p_z, x, p_x$  and the independent length parameter  $s$ . 2d densities are obtained from projections of  $f$  to the  $z, x$  plane. They are represented as spline series and must be stored, at least until they can not longer communicate by light rays with later evaluation points. 3d charge and current densities are obtained from the 2d densities and by extension with a fixed distribution  $H(Y)$  that describes a time independent vertical profile, with  $Y$  the vertical lab-frame coordinate. Shielding by parallel horizontal conducting planes can be considered by mirror charges. The 2d electromagnetic fields  $E_z(Z, X, t)$ ,  $E_x(Z, X, t)$ ,  $B_y(Z, X, t)$  in lab frame coordinates  $Z, X$  and time  $t$  are the 3d fields weighted with the vertical density. Solving the retardation integrals is the main effort of the method. The fields are calculated on a grid and interpolated to every required position. The integration of Vlasov equation is described in [3].

### Sub-Bunch-Approach

This approach uses a set of sub-bunches with well defined shape and trajectory to define 3d source distributions  $\rho(\mathbf{r}, t)$ ,  $\mathbf{J}(\mathbf{r}, t)$  in the present and the past. Therefore the trajectories have to be known back in time. Test particles are tracked under the influence of external and sub-bunch fields. The tracking takes into account self interactions if the motion of sub-bunches and test particles is coupled, i.e., if a test particle defines a sub-bunch trajectory. Since the field of each 3d source sub-bunch has (in principle) to be calculated for every test position by a 3d integration of retarded sources, the full field computations is quite time consuming. This can be improved by efficient calculation techniques for sub-bunches (reducing the effort of one-to-one interactions) and by mesh techniques (reducing the number of field calculations).

*Sub-bunch calculations:* For spherical Gaussian sub-bunches the 3d integration can be reduced to a 1d integral [5]. The codes TraFiC<sup>4</sup> [6] and CSRtrack [7] adopt a different calculation method that also reduces the dimension of the field integral [8]. A certain type of 3d distribution can be represented by the convolution of a longitudinal 1d profile  $\lambda(s, t)$  with a transverse 2d density function  $\eta(x, y)$ . The electromagnetic field can be written in the same way as convolution of the field of the 1d source with the transverse density. The 1d source needs a 1d integration and the 2d convolution integral in vicinity of

field singularities at the 1d trajectory is approximated efficiently with help of few auxiliary functions.

Two types of *mesh techniques* can be used and combined. The ‘em’-mesh discretizes the volume with all test point *where* the field is needed. The so called Green’s function approach estimates the field of all sub-bunches that are on individual trajectories by the fields  $\mathbf{E}^{(0)}(\mathbf{r}, t_0)$ ,  $\mathbf{B}^{(0)}(\mathbf{r}, t_0)$  of a reference sub-bunch that travels along a reference trajectory  $\mathbf{r}_0(t)$ . These fields are evaluated on the ‘g’-mesh (‘g’ for Green’s). At the observation time  $t_0$  the trajectory  $\mathbf{r}_\nu(t)$  of sub-bunch  $\nu$  is approximated by a shift- and rotation-transformation  $(\mathbf{r}_\nu(t_0), \mathbf{R}_\nu)$  of the reference trajectory  $\mathbf{r}_\nu(t) \approx \mathbf{r}_\nu(t_0) + \mathbf{R}_\nu \cdot (\mathbf{r}_0(t) - \mathbf{r}_0(t_0))$ . The same transformation is applied to the electromagnetic fields. CSRtrack uses 2d meshes. A qualitative diagram with the scaling of the numerical effort with the number of particles is shown in Fig. 2.

*History of trajectories:* TRAFIC<sup>4</sup> stores the trajectory of all sub-bunches in the past, as it is needed for the computation of retarded sources. This complicates the coding and later restarts of tracking calculations. CSRtrack approximates recent densities by back tracking without self forces from the present state.

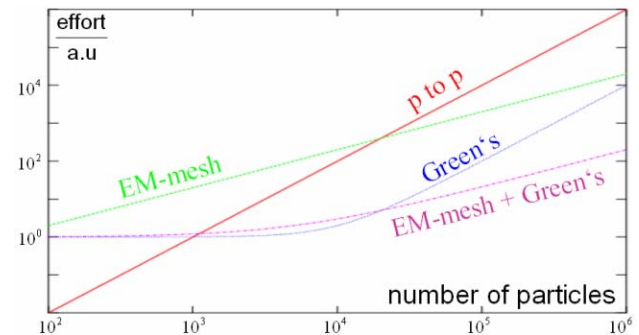


Fig. 2: Numerical effort of different mesh techniques.

### 1D or Projected Approach

The 1d approach uses a simplified model for the calculation of longitudinal forces [9,5]. The implementations are very efficient but the approach neglects a couple of physical effects: it ignores transverse forces as well as transverse beam dimensions and assumes that the longitudinal distribution is unchanged at retarded times. A ‘renormalized’ Coulomb term is used to extract the field singularity in the 1d beam.

The particle distribution is projected to the reference trajectory and a smooth one dimensional charge density  $\lambda(s)$  is calculated by binning or filtering. The smoothing is crucial for the stability and accuracy of the simulation because the micro bunch instability is sensitive to high frequency components in the charge density.

The longitudinal field  $E^{(\lambda)}$  can be calculated by one dimensional integration

$$E^{(\lambda)}(s_0, t_0) = \int \lambda'(u + s_0 - vt_0) K(s_0, u) du,$$

with the kernel function  $K(s_0, u)$  that depends on the geometry of the trajectory. This integral is a convolution in time.

### Approach with Paraxial Approximation

T. Agoh and K. Yokoya [10] use an approach that is complementary to the methods described above. It is based on the mesh discretization of a partial differential equation. The truncation of the mesh is related to the shielding by a beam pipe. The method is based on the assumptions that the pipe radius is much smaller than the bending radius, that the field propagation backward can be ignored (paraxial approximation) and that  $\gamma \gg 1$ . The curvature of the trajectory needs not to be constant and resistive wall effects can be taken into account. The paraxial approximation allows adiabatic changes of the pipe geometry and even tapers, given that the stimulation of backward waves is negligible.

For the derivation of the PDE the electrical field  $\mathbf{E}(\mathbf{r}, t)$  is written in accelerator coordinates  $\sum_{\xi=x,y,s} \tilde{E}_{\xi}(x, y, s, t) \mathbf{e}_{\xi}$

with  $x, y$  the transverse- and  $s$  the length coordinate. The Fourier transformed component

$$E_{\xi}(x, y, k, s) = \int \tilde{E}_{\xi}(x, y, s, s + \tau) \exp(-ik\tau) d\tau$$

varies slowly in  $s$ . With  $\partial_s^2 E_{\xi} \ll 2ik \partial_s E_{\xi}$  and the assumptions mentioned above, the paraxial approximation for transverse field components follows as

$$\partial_s E_{\perp} = \frac{i}{2k} \left[ (\nabla_{\perp}^2 + 2k^2 x/\rho) E_{\perp} - \mu_0 \nabla_{\perp} J_0 \right].$$

$\rho$  is the local curvature radius and  $J_0$  the charge density. The PDE is discretized on a 3d mesh by a finite difference scheme and integrated along the  $s$  axis by a leap frog schema.

### Zeuthen Benchmark Chicane

A simple four-bend chicane was proposed on an ICFA mini workshop [11] as benchmark case for CSR codes. The benchmark problem was and is investigated with 1d- and sub-bunch-codes. Calculations with the Vlasov-Maxwell approach have been published.

Most investigations have been done for the 5 GeV case with a 1 nC Gaussian bunch. The 1d- and sub-bunch methods agree on a few percent growth of the horizontal slice emittance and a 50% growth of the projected emittance but there is a significant difference in the relative energy loss obtained by all 1d codes ( $\approx 0.04\%$ ) to the results of the sub-bunch methods ( $\approx 0.06\%$ ). The Vlasov-Maxwell calculation confirms the result of the sub-bunch methods [3,4]. The spread of the non-1d results of about 10% is probably related to the modeling of the transverse shape of the distribution.

The low energy case (500 MeV) is more challenging as the interference of the compression process with self forces is much stronger. So far it was considered only by few CSR codes. The results of different methods deviate stronger. E.g. the 1d approach without space charge calculates only 50% of the projected emittance obtained by a sub-bunch method [12].

## PART II: SIMULATION OF BC SYSTEMS\*

A couple of physical and/or numerical problems have to be considered for the realistic simulation of bunch compression systems. For example, the typically  $10^{10}$  electrons in a bunch have to be represented by a distribution of much less macro particles or by a density function.

Physical is the problem of shot noise in the electron distribution that can be amplified by many orders of magnitude. A small modulation in density is converted by longitudinal SC and/or CSR impedances to a small energy modulation which causes longitudinal displacements in dispersive sections. This leads for a certain range of wavelength to a  $\mu$ -bunching amplification. The real effect is controlled by additional hardware (the "laser heater") that increases the uncorrelated energy spread.

A numerical simulation of  $\mu$ -bunching effects is still beyond the resolution of most tracking programs. Therefore the problem is split into a separate investigation of  $\mu$ -bunching effects [13,14,15] and of pure macroscopic effects. *Noise suppression* strategies are important for the numerical field calculations and the treatment of particle distributions.

*Space charge effects* contribute significantly to the longitudinal phase space before and after the compression. In the case of a 'controlled compression' with phase space linearization the shape of the compressed bunch depends *very sensitive* on nearly every effect (e.g. wakes) and every parameter (e.g. bunch charge). The simulation of BC systems involves the use of several codes and tools for the calculation of linear and dispersive sections, for the treatment of wakes and for *phase space conversions*.

### Particle Distributions

To avoid a loss of information it is desirable to use the same particle distribution for the simulation of all sections, in the ideal case from start to end. Typical injector simulations are done with  $\sim 10^5 \dots 10^6$  equi-charged macro particles that are random or semi-random distributions in 6d phase space. Even for distributions with more particles the noise is critical. In 1d methods it can be controlled by careful use of binning, filtering and density-adaptive techniques. For mesh based field calculations the number of particles per cell has to be sufficient. The balance between resolution and particle number is delicate. Sometimes a reduction of the dimension allows approximations with better signal to noise ratio (e.g. rotational symmetry for SC effects or horizontal distributions with effective vertical dimension for CSR codes). A technique used for CSR calculations is the creation of a second distribution that keeps essential properties of the original distribution but is smooth. The smooth distribution is tracked with self interactions and produces the electromagnetic fields that affect the original

\* BC systems may include several compressors and linac sections.

distribution which is not field generating. Further tracking is continued with the original distribution.

### Non-linear Longitudinal Effects in a BC Chicane

The qualitative behavior of the longitudinal phase space without (red) and with (blue) compensation of non-linear effects is shown in Fig. 3. Non-linear effects are caused by the cosine time dependency of the rf and by higher order dispersion in the chicane. This leads to a rollover in phase space and a sharp spike in the current distribution for the uncompensated case. The current is increased by a factor inverse proportional to the uncorrelated energy spread. The blue phase space distribution in the left diagram has a positive 2<sup>nd</sup> derivative and differs less from the linear correlation (in black). The overcompensation is achieved with a higher harmonic rf system and leads to a more uniform compression. If a rollover is avoided, the compression factor depends sensitively on the shape of the energy-length correlation and the dispersion.

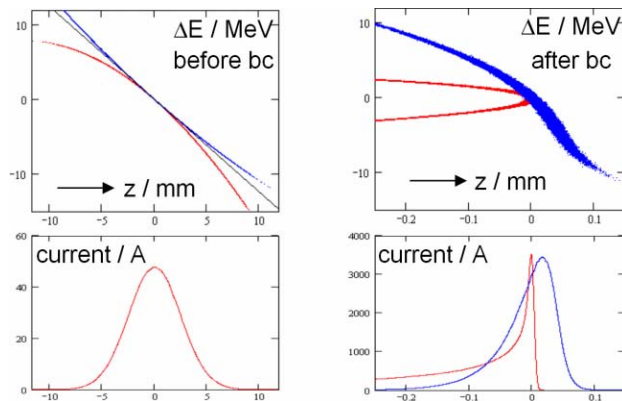


Fig. 3: Controlled- (blue) and rollover- (red) compression. (Idealized example without self-effects.)

### Example “rollover-compression” (FLASH)

The schematic layout of the FLASH facility at DESY can be seen in Fig. 4. Bunches of typically 1 nC are generated in a laser driven RF gun. The beam is accelerated to ~125 MeV by a TESLA module with 8 cavities. The chirp is created by off-crest operation of the last four cavities. A pre-compression with slight rollover is achieved in a C-type chicane. The second compression is done at 380 MeV with an S-type compressor after two more modules that accelerate on crest.

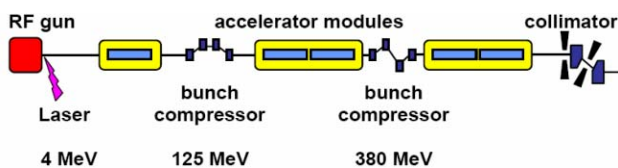


Fig. 4: Schematic layout of the FLASH BC system.

Fig. 5 shows intermediate results of a start to end simulation using ASTRA, CSRtrack-1d and GENESIS. The color coding indicates the injection time and helps to understand the dynamic of compression. The upper plot has approximately the rollover shape as in the idealized Fig. 3, but with few particles in the lower branch. The

‘horn’ at the rollover point with significantly increased energy is due to space charge forces *after* the 1<sup>st</sup> compression. CSR effects are small compared to that. The distribution after the 2<sup>nd</sup> compressor can be seen in the lower plot. The initial negative length-energy correlation of the green particles results in a longitudinal position close to the rollover point. The distortions are caused by CSR. The blue particles are decompressed due to the (essentially) positive slope of the initial chirp. After both compressors the 0.5 nC bunch produces a current spike of approximately 1.2 kA. Space charge effects *after* the 2<sup>nd</sup> compressor produce a second horn that affects the longitudinal dynamic in the collimator if the gradient in the last two modules is weak (e.g. 440 MeV beam energy for 30 nm FEL radiation).

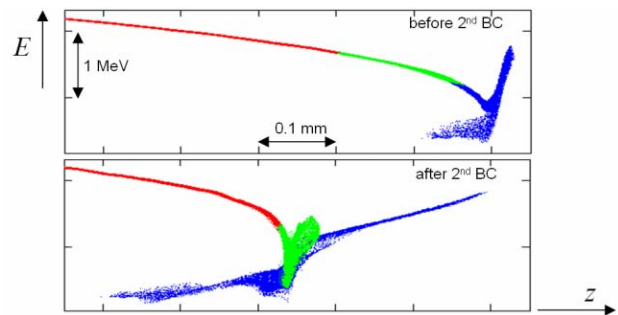


Fig. 5: Simulation of long. phase space of FLASH.

### Example “controlled compression” (E. XFEL)

The European XFEL uses a controlled compression in two stages to increase the initial current of ~ 50 A of a 1 nC bunch to 5 kA. After the laser gun and one TESLA module that accelerates on crest to ~ 130 MeV follows a linac with four fundamental mode modules and two modules with 3<sup>rd</sup> harmonic cavities. Four degrees of freedom (amplitudes and phases at both frequencies) are used to adjust the energy, the chirp and to manipulate higher order non-linearities. The 1<sup>st</sup> compression at 500 MeV increases the current to 1 kA. The linac before the second compressor accelerates to 2 GeV (with weak influence on the chirp). Both compressors are C-type chicanes with identical magnets and drift length followed by diagnostic sections. The energy after the main linac is typically 17 – 18 GeV.

Start to end simulations have been done with ASTRA and CSRtrack (sub-bunch) for the system below 3 GeV. The rest was simulated with ELEGANT and GENESIS. Longitudinal SC fields above 3 GeV have been considered by a semi-analytic approach. The currents in Fig. 6 and the longitudinal phase space distributions in Fig. 7 represent some results of the full simulation.

The longitudinal phase space distribution directly after BC2 is comparable to the controlled compression in Fig. 3. The slight rollover at both sides of the bunch produces no spikes but shoulders according to the low charge density and high energy spread of that part of the bunch. The uncorrelated spread in the core is 1 MeV which is precisely the product of the compression factor and the uncorrelated energy spread induced by a laser heater after

the 1<sup>st</sup> module. The normalized slice emittances in the core are increased by few percent, the horizontal slice emittance in the leading edge is increased from 0.65  $\mu\text{m}$  to 0.75  $\mu\text{m}$ .

The longitudinal phase space after the main linac is altered by cavity wakes and by space charge effects. The wakes compensate a large part of the energy chirp that was needed for the compression. Despite the high particle energy of 2 GeV the longitudinal space charge forces are strong enough to induce a positive correlation between position and energy with a slope of  $\sim 0.5 \text{ MeV}/\mu\text{m}$ .

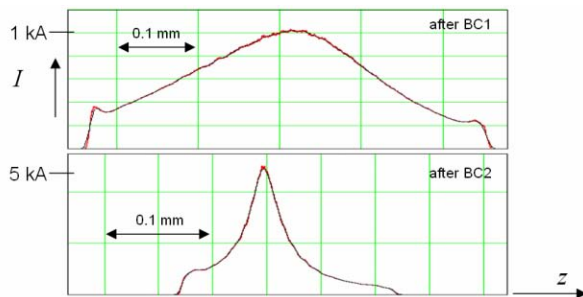


Fig. 6: Current after BC1 and BC2 in Eu. XFEL.

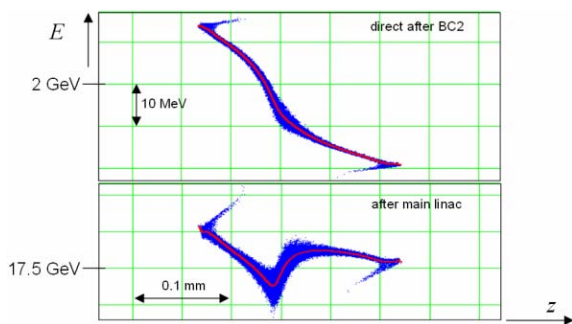


Fig. 7: Phase space simulation for European XFEL.

### Compensation of Effects in BC Systems

This problem is addressed to demonstrate that unwanted effects from one BC chicane can interfere constructively or destructively with effects from a second chicane. The case of (partial) compensation might be a design goal but it means that the net effect is a difference of larger individual effects or numerically spoken the difference of large numbers. Therefore the simulation of a coupled system needs higher precision than necessary for individual components or otherwise predictions might be uncertain or worse case estimations too pessimistic.

For example the compression ratios, chirps and  $r_{56}$  values in the two BC system of the European XFEL are chosen so that the projected emittance after both BCs is increased a factor between 1.2 and 3.5 dependent on the optical phase advance between both stages [16]. This result assumes free space conditions. But: it is difficult or impossible to avoid *shielding effects* in both compressors completely. (The shielding condition for the CSR *after* a bending magnet is  $5L_d \ll h^2/\sigma$  with  $L_d$  the length of the drift,  $h$  the gap width and  $\sigma$  the bunch length.) For long drifts even resistive wall wakes can contribute considerably.

## CONCLUSION AND OUTLOOK

The calculation of effects in BC systems is a challenging task, especially if the interference of effects from individual stages defines the performance of the full system. The methods for the calculation of effects on non-linear trajectories have been extended. Nearly all important physical effects (SC, CSR, shape variation, resistive walls) are covered by an approach. The resolution in phase space (e.g. number of macro-particles) has been increased but is still not sufficient to compute  $\mu$ -bunch effects in a full-bunch simulation. A code that combines the strengths of the existing approaches and treats SC, CSR, shape variation and resistive shielding *together* seems to be in reach.

## REFERENCES

- [1] E.Saldin et al., 'Expected Properties of Radiation from VUV-FEL at DESY (Femtosecond Mode of Operation)', Proceedings FEL Conf. 2004, p 212-215.
- [2] K.Flöttmann et al., 'Generation of Ultrashort Electron Bunches by cancellation of non-linear distortions in the longitudinal phase space', TESLA-FEL-2001-06.
- [3] G.Bassi, J.A.Ellison, B.Warnock, 'Vlasov Treatment of CSR from Arbitrary Planar Orbits', PAC 2004.
- [4] G.Bassi et al., 'Progress on a Vlasov Treatment of CSR from Arbitrary Planar Orbits', PAC 2005.
- [5] M.Dohlus, 'Two Methods for the Calculation of CSR Fields', TESLA-FEL-2003-05.
- [6] T.Limberg, A.Kabel, M.Dohlus, 'Numerical Calculation of CSR Effects Using TraFiC4', NIM A455 (2000) 185-189.
- [7] M.Dohlus et al., 'CSRtrack: Faster Calculations of 3-d CSR Effects', Proceedings FEL Conf. 2004, p 18-21.
- [8] M.Dohlus et al., 'Efficient Field Calculation of 3-D Bunches on General Trajectories', NIM A445 (2000) 338-342.
- [9] E. Saldin et al., 'Radiative Interaction of Electrons in a Bunch Moving in an Undulator', NIM A417 (1998) 158-168.
- [10] T.Agoh, K.Yokoya, 'Calculation of coherent synchrotron radiation using mesh', Phys.Rev. ST AB, 7, 054403 (2004).
- [11] ICFA Beam Dynamics Mini-Workshop on CSR, Berlin-Zeuthen, 2002, (<http://www.desy.de/csr>).
- [12] G.Bassi et al., 'Overview of CSR Codes', NIM A557 (2006) 189-204.
- [13] E.Saldin et al., 'Klystron instability of a relativistic electron beam in a bunch compressor', NIM A490 (2002) 1-8.
- [14] E.Saldin et al., 'Longitudinal Space Charge Driven Microbunching Instability in TTF2 linac', TESLA-FEL-2002-02.
- [15] Z.Huang et al., 'Microbunching instability due to bunch compression', ICFA Beam Dynamics Newsletter, No. 38, Dec 2005, p37 - 51.
- [16] Dohlus, Limberg, 'Impact of optics on CSR-related Emittance Growth in BC Chicanes', PAC2005.